

# Quantitative analysis of peri-tumor tissue elasticity based on shear-wave elastography for breast tumor classification

Yang Xiao, Jie Zeng, Ming Qian, Rongqin Zheng and Hairong Zheng, *Senior Member, IEEE*

**Abstract**—For shear-wave elastography (SWE) images, the most common site of tumor-associated stiffness is generally in the surrounding stroma rather than the tumor itself. The aim of this study is to assess the value of the peri-tumor tissue elasticity in the classification of breast tumors. SWE images of 106 breast tumors (65 benign, 41 malignant) were collected from 82 consecutive patients. By applying the image processing method, 5 elastographic features of the peri-tumor area (elasticity modulus mean, maximum, standard deviation, hardness degree and elasticity ratio) were computed to represent peri-tumor tissue elasticity. B-mode Breast Imaging Reporting and Data System (BI-RADS) were used for comparing the diagnostic performances between the grayscale US and color SWE images. Histopathologic results were used as the reference standard. The t-test, point biserial correlation coefficient and receiver operating characteristic (ROC) curve analysis were performed for statistical analysis. As a result, the  $A_z$  values (area under ROC curve) were 0.92, 0.95, 0.94, 0.91, and 0.98 for the classifiers using the five elastographic features respectively, and 0.91 for BI-RADS assessment. The results showed that the peri-tumor tissue elasticity could provide valuable information for breast tumor classification.

## I. INTRODUCTION

Shear-wave elastography (SWE) has recently been developed as a quantitative elastography technique based on the combination of an acoustic radiation force created by a focused ultrasound beam and an ultrafast imaging sequence capable of catching the propagation of the resulting shear waves. The local shear wave velocity is recovered, enabling the construction of a two-dimensional map of elasticity modulus [1-2]. Some pathological cases, such as breast tumors, lead to considerable changes in soft tissue structure, modifying its elastic properties and substantially resulting in increased stiffness. This property serves as the basis for elastography in differentiating malignant from benign breast tumors [3]. For SWE images, many malignant tumors are not uniformly stiff, and the maximum areas of stiffness are always found in the peri-tumor stroma rather than the tumor itself [4-5]. Until recently the published literatures with SWE mostly focus on the stiffest area on the color maps whether it is within or adjacent to the tumor [3-5]. Quantitative analysis of the peri-tumor area with SWE images has the potential to

provide critical information for distinguishing malignant and benign breast tumors in order to avoid unnecessary biopsy.

This study proposed several quantitative elastographic features of the peri-tumor tissue by using SWE image processing method, and evaluated their values for breast tumor classification. The diagnosis performance was validated by correlating the results with the diagnosis assessed by Breast Imaging Reporting and Data System (BI-RADS) and histopathologic examination [6].

## II. MATERIALS AND METHODS

### A. Patients and Image Acquisition

The study group consisted of patients with visible breast abnormalities on routine B-mode scans. 106 breast tumors (65 benign, 41 malignant) of 82 consecutive women (mean age, 43 years; age range, 16-75 years) were collected. The tumor sizes determined on B-Mode images ranged from 0.4 to 3.2 cm (mean size, 1.3 cm). The malignant tumors included 32 cases of invasive ductal carcinoma, 2 cases of invasive lobular carcinoma, 4 cases of invasive papillary carcinoma and 3 cases of ductal carcinoma in situ (DCIS). The benign tumors included 42 cases of fibroadenoma, 4 cases of papilloma, 5 case of cystosarcoma phylloides and 13 cases of fibrocystic change.

SWE and B-mode US images of breasts were performed using an Aixplorer scanner (SuperSonic Imagine, Aix en Provence, France) equipped with a 4-15 MHz linear array broadband probe. For elastographic images, a ROI box was set centered on the target lesion and peri-tumoural areas were adequately imaged (including sufficient normal tissue). After a standard scan, both elastographic and B-mode images were displayed at the same time on a monitor, with the elastographic image on the top and the B-mode image on the bottom. The elastographic images were displayed with the use of 256-color mapping for each pixel according to the value of elasticity modulus. Two or three sonoelastographic images were captured per case and all these images were saved as DICOM files in a hard disc.

### C. BI-RADS Assessment

B-mode US images initially underwent BI-RADS classification by 2 skilled radiologists who were blinded to the elastography findings and pathologic results. BI-RADS features and visual assessments (category 2, benign; category 3, probably benign; category 4a, low suspicion; category 4b, intermediate suspicion; category 4c, moderate suspicion; category 5, highly suggestive of malignancy) were recorded.

\*Research supported by National Natural Science Foundation of China (81027006)

First Author Yang Xiao and corresponding author Hairong Zheng are with the Paul C. Lauterbur Research Center for Biomedical imaging, Shenzhen Institute of Advanced Technology, Chinese Academy of Sciences, Shenzhen, China 518055 (corresponding author to provide phone: +86-755-86392272; fax: +86-755-86392299; e-mail: hr.zheng@siat.ac.cn)

Jie Zeng and Rongqin Zheng are with Department of Medical Ultrasonics, Third Affiliated Hospital of Sun Yat-Sen University, Guangzhou, China 510630(e-mail: zhengrongqin@hotmail.com).

#### D. Reference Standard

All breast tumors were subjected to core biopsy or fine needle aspiration cytology for histopathologic diagnosis and histopathologic results were used as reference standard.

#### E. Quantitative Elastographic Features Generation

To obtain the elastographic features automatically and objectively, a three-step process is performed, including elasticity data reconstruction, automatic segmentation, and feature extraction.

**Elasticity data reconstruction.** For Aixplorer scanner, the top part is a combination of B-mode and SWE images (Figure.1 (a)), while the bottom part is the original B-mode image. The original color elasticity image can be obtained by subtracting the original B-mode image from the combined image, but still in RGB format (Figure.1 (b)). According to the principle of color SSI image, the color bar, displayed on the right of image, represents elasticity modulus value from 0 to the maximum measurement range (Figure.1 (c)), which can be used for decoding. In this method, the color line is divided into 2200 color classes from blue to red and their RGB values are recorded respectively. Each pixel of the color elasticity image is compared to all the color classes, and the distance between the pixel and each color class is defined as:

$$d(m) = \sqrt{(R_{\text{pixel}} - R_m)^2 + (G_{\text{pixel}} - G_m)^2 + (B_{\text{pixel}} - B_m)^2} \quad (m = 1, 2, 3, \dots, 2200) \quad (1)$$

where the subscripts  $\text{pixel}$  and  $m$  denote the pixel and color class, R, G and B are their red, green and blue values respectively. Once the minimum  $d_{\min}$  is found, its corresponding elasticity modulus value is regarded as the reconstructed elasticity data of this pixel. After performing a pixel by pixel reconstruction, the original color elasticity image is transformed from RGB space into a matrix of tone of grey, whose values vary from 0 to the maximum range (Figure.1 (d)). We confirm that the transformation is valid by comparing the original image (Figure.1 (a)) and the re-decoded image (Figure.1 (e)), which is obtained by changing the greyscale elasticity image into RGB format and superimposing it on the original B-mode image.

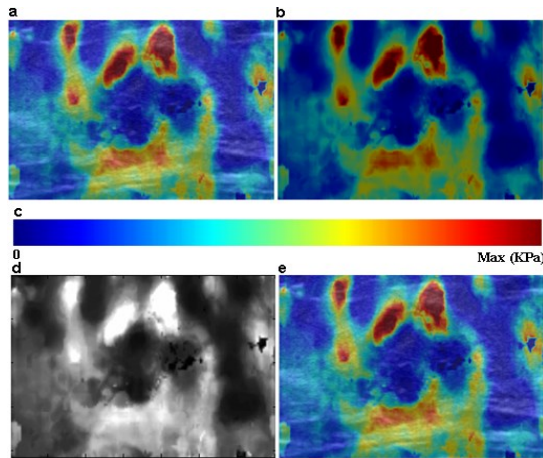


Figure.1. (a) Combination of B-mode and elastographic images from Aixplorer scanner, (b) Original color elasticity image, (c) Color line, (d) Reconstructed greyscale elasticity image, (e) Re-decoded image.

**Automatic segmentation.** Since the color SWE image is difficult to extract the real tumor contour directly, the greyscale B-mode image is used for automatic segmentation. In this study, a segmentation method using active contour model based on Mumford–Shah function and level sets is proposed [7]. Then a morphological closing algorithm is applied to remove small holes inside the segmented tumor. The results of the proposed automatic segmentation method were presented in Figure.2(a). After the automatic segmentation of the tumor on B-mode image, the extracted tumor contour is then mapped to the corresponding greyscale elasticity image for the following calculation of tumor statistics (Figure.2 (b)).

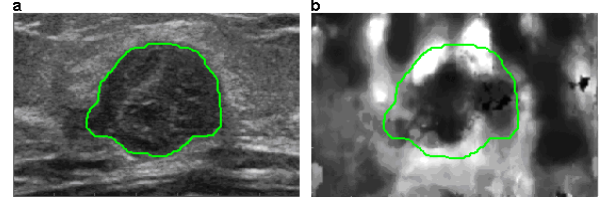


Figure.2. (a) The contour of the segmented tumor on the B-mode image, (b) The contour of the segmented tumor mapped on the elasticity image

**Feature extraction.** Many malignant breast tumors are not uniformly stiff but have a halo of peri-tumoral stromal stiffness on SWE images, therefore, elastographic features of the peri-tumor area are calculated and evaluated in this study. First, a morphological dilation algorithm is applied to create the peritumoral area outside the segmented tumor, with a disk structuring element of 35-pixel diameter. As seen in Figure.3 (a), the area between the green line (tumor contour) and the white line is regarded as the region of interest.

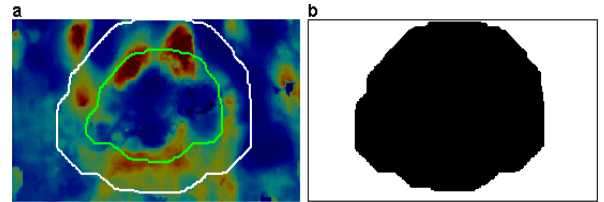


Figure.3. (a) The peritumoral area on the color elasticity image, which is between the green line and the white line (b) The rest area created by subtracting the abnormal area from the whole ROI, which is represented by white color.

Then five elastographic features of the peri-tumor area are quantified, including mean elasticity modulus, the maximum elasticity modulus, standard deviation, hardness degree, and elasticity ratio ( $PE_{\text{mean}}$ ,  $PE_{\text{max}}$ ,  $PE_{\text{std}}$ , PHD and  $PE_{\text{ratio}}$ ).

The  $PE_{\text{mean}}$ ,  $PE_{\text{max}}$  and  $PE_{\text{std}}$  are respectively determined by calculating the reconstructed elasticity values of pixels within the peri-tumor area:

$$PE_{\text{mean}} = \frac{\sum_{(i,j) \in \text{peritumor}} E(i,j)}{N_{\text{peritumor}}} \quad (1)$$

$$PE_{\text{max}} = \max_{(i,j) \in \text{peritumor}} (E(i,j)) \quad (2)$$

$$PE_{\text{std}} = \sqrt{\frac{1}{N_{\text{peritumor}} - 1} \sum_{(i,j) \in \text{peritumor}} (E(i,j) - PE_{\text{mean}})^2} \quad (3)$$

where  $E(i, j)$  is the elasticity value of pixel  $(i, j)$ , and  $N_{peritumor}$  is the number of pixels within the peri-tumor area.

The hard pixel is defined if its elasticity value is larger than a threshold. The PHD is given using the following formula:

$$PHD = \frac{N_{hard}}{N_{peritumor}} \times 100 \% \quad (4)$$

where  $N_{hard}$  is the number of hard pixels within the peri-tumor area.

To obtain elasticity ratio ( $PE_{ratio}$ ) automatically and objectively,  $PE_{ratio}$  is defined as:

$$PE_{ratio} = \frac{PE_{mean}}{PRE_{mean}} \quad (5)$$

where  $PRE_{mean}$  denotes the mean elasticity value of the rest area created by subtracting the abnormal area (including both the tumor and the peri-tumor area) from the whole ROI (Figure.5 (b)). It is important that the ROI should consist of adequate normal tissue to compute valid  $PE_{ratio}$  value.

#### F. Statistical Analysis

Differences between the values of the five features for the benign and malignant tumors respectively were compared using t test. The relationship between pathologic result and each feature was evaluated by point biserial correlation coefficient ( $r_{pb}$ ). Diagnostic performances of the classifiers based on each elastographic feature and BI-RADS assessment were evaluated with accuracy, sensitivity, specificity, positive (PPV) and negative predictive values (NPV), and ROC curve, respectively. The differences between the  $A_z$  values of the two classifiers were compared using z-test.  $P < 0.05$  was considered to indicate a statistically significant difference. The ROC analysis was performed by using the ROCKIT software. Statistical analyses other than ROC analysis were performed by using SPSS version 19.0 software [8].

$PE_{ratio} = 0.82$ .

### III. RESULTS

#### A. Performance of BI-RADS

The visual assessment of 106 solid breast tumors based on B-mode US images was as follows: category 2 in 2 cases (malignant, 0% [0 of 2]), category 3 in 48 cases (malignant, 6.3% [3 of 48]), category 4a in 14 cases (malignant, 42.9% [6 of 14]), category 4b in 17 cases (malignant, 58.8% [10 of 17]), category 4c in 13 cases (malignant, 76.9% [10 of 13]), and category 5 in 12 cases (malignant, 100% [12 of 12]).

Considering category 4a or higher as test positive for malignancy, overall accuracy of BI-RADS classification was 83.0% (88 of 106); Sensitivity was 92.7% (38 of 41); Specificity was 76.9% (50 of 65); PPV was 71.7% (38 of 53); and NPV was 94.3% (50 of 53). The  $A_z$  value was 0.91 (95%CI: 0.84, 0.96) for BI-RADS assessment ( $p < 0.01$ ).

#### B. Performance of Peri-tumor Elastographic Features

For the peri-tumor area, the mean values of the five elastographic features were significantly different between benign and malignant tumors using t test ( $p < 0.01$ ) (Table 1). The peri-tumoral regions of benign masses (Figure.4) were softer than those of malignancies (Figure.5) with  $PE_{mean}$  of  $16.28 \pm 7.21$  kPa compared with  $44.51 \pm 20.48$  kPa. The  $PE_{max}$  also represents the stiffness of the peri-tumor area, and the mean  $\pm$  SD was  $46.67 \pm 19.48$  kPa for the benign tumors and  $139.34 \pm 50.26$  kPa for the malignancies. Malignant tumors showed higher level of heterogeneous elasticity with the  $PE_{std}$  of  $31.12 \pm 16.71$  compared with  $7.97 \pm 4.07$  of benign tumors. In this paper,  $T_{hard}$  was defined as 50, and thereby the values of PHD were equal to 0 in 39 benign cases (60.0% [39 of 65]). The  $PE_{ratio}$  are significant in classifying between benign and malignant tumors ( $p < 0.01$ ), and the point biserial correlation coefficient between pathologic result and  $PE_{ratio}$  was up to 0.75, conforming to the predictions that the peri-tumor stiffness of the malignancies were harder than the surrounding normal tissue.

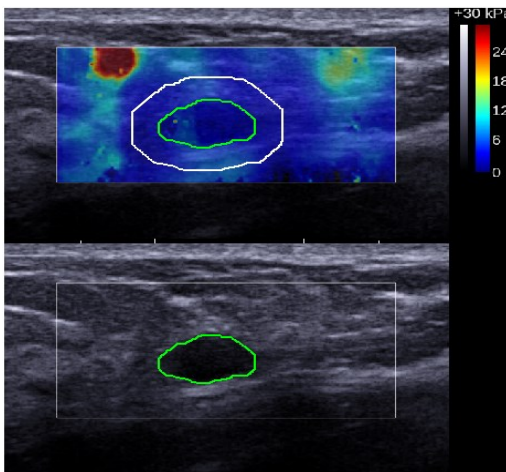


Figure.4. A fibroadenoma considered to be BI-RADS category 3 in a 49-year-old woman. Top: SSI elasticity image. Bottom: B-mode US image. In this case,  $PE_{mean} = 4.3$  kPa,  $PE_{max} = 9.5$  kPa,  $PE_{std} = 1.4$ ,  $PHD = 0$ , and

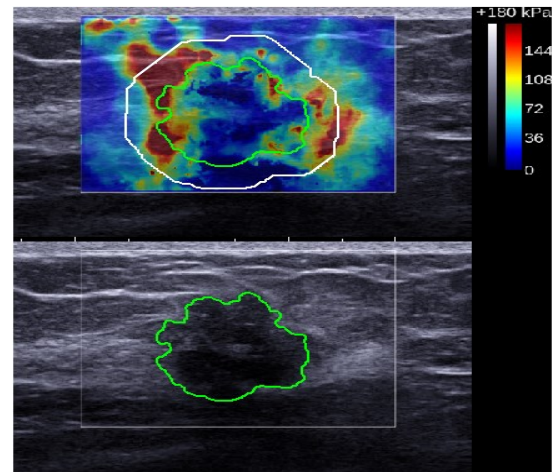


Figure.5. An invasive ductal carcinoma considered to be BI-RADS category 5 in a 36-year-old woman. Top: SSI elasticity image. Bottom: B-mode US image. In this case,  $PE_{mean} = 140$  kPa,  $PE_{max} = 180$  kPa,  $PE_{std} = 48.7$ ,  $PHD =$

0.58, and  $PE_{ratio} = 2.10$ .

Once the optimal cutoff points of the five features were determined by Youden index (Table 1) respectively, accuracy, sensitivity, specificity, PPV and NPV values of the classifiers based on these elastographic features were calculated and listed in Table.2. All the elastographic features provides higher specificity than BI-RADS assessment without loss of sensitivity. Especially for the  $PE_{ratio}$ , the  $A_z$  value (0.98) was higher than the  $A_z$  value of BI-RADS assessment (0.91). By using z-test, the difference of  $A_z$  values was statistically significant ( $z = 2.24 > 1.96$ ,  $p = 0.02 < 0.05$ ).

TABLE I. THE MEAN VALUE, STANDARD DEVIATION, CUTOFF VALUE, P VALUE, CORRELATION COEFFICIENT  $r_{pb}$  OF ELASTOGRAPHIC FEATURES IN THE BENIGN AND MALIGNANT CASES

Feature	BENIGN		MALIGNANT		Cvalue	p value	$r_{pb}$
	Mean ± SD	Mean ± SD	Cvalue	p value			
$PE_{mean}$	16.28 ± 7.21	44.51 ± 20.48	32.0	<0.01	0.703		
$PE_{max}$	46.67 ± 19.48	139.34 ± 50.26	90.0	<0.01	0.791		
$PE_{std}$	7.97 ± 4.07	31.12 ± 16.71	13.0	<0.01	0.721		
PHD	0.02 ± 0.04	0.27 ± 0.23	0.03	<0.01	0.699		
$PE_{ratio}$	1.00 ± 0.22	1.94 ± 0.58	1.30	<0.01	0.751		

TABLE II. THE ACCURACY, SENSITIVITY, SPECIFICITY, PPV, NPV,  $A_z$ , Z AND P VALUE OF BI-RADS ASSESSMENT AND ELASTOGRAPHIC FEATURES

	BI-RADS	$PE_{mean}$	$PE_{max}$	$PE_{std}$	PHD	$PE_{ratio}$
Accuracy (%)	83.0	78.3	91.5	90.6	87.7	92.4
Sensitivity (%)	92.7	70.7	80.5	87.8	87.8	92.7
Specificity (%)	76.9	98.5	98.5	92.3	87.7	92.3
PPV (%)	71.7	96.7	97.1	87.8	81.8	88.4
NPV (%)	94.3	84.2	88.9	92.3	91.9	95.2
$A_z$	0.91	0.92	0.95	0.94	0.91	0.98
z		0.09	1.06	0.88	0.14	2.24
p value		0.92	0.29	0.38	0.89	0.02

#### IV. DISCUSSION AND CONCLUSION

Considering the most common site of tumor-associated stiffness at SWE image is usually in the surrounding stroma rather than the tumor itself. In this study, five features representing the elasticity of the peri-tumor area are quantified and evaluated. Figure 6 compares the behavior of ROC curves for the BI-RADS assessment based on the conventional grayscale US and the peri-tumor elastographic features based on SWE images. The area under the ROC curves ( $A_z$ ) values were 0.92, 0.95, 0.94, 0.91, and 0.98 for the  $PE_{mean}$ ,  $PE_{max}$ ,  $PE_{std}$ , PHD, and  $PE_{ratio}$  respectively, and 0.91 for BI-RADS assessment. It can be concluded that the elasticity information of the peri-tumor area may be more sensitive and accurate in breast tumor characterization compared with BI-RADS classification. Especially for the  $PE_{ratio}$ , the difference of  $A_z$  values was statistically significant, which showed that the method that only used the  $PE_{ratio}$  can provide more accurate diagnosis than the BI-RADS using conventional US. This finding results from benign tumors generally with smooth borders and that the benign tumors are loosely bound to the surrounding tissues, whereas malignant tumors are usually characterized by firm desmoplastic reactions with the

surrounding tissue [9].

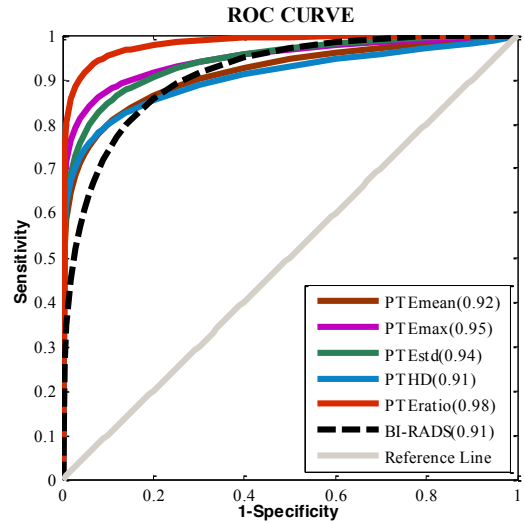


Figure.6. Comparison of ROC curves for BI-RADS assessment (dashed line) and the elastographic features of the peri-tumoral area (solid line).

In conclusion, the proposed method can acquire elastographic features of peri-tumor tissue from SWE images automatically and objectively, and provide satisfactory performance in differentiating malignant and benign breast tumors. The peri-tumor tissue elasticity has the potential to be a valuable tool in addition to diagnostic ultrasonography.

#### ACKNOWLEDGMENT

The work was supported by National Basic Research Program 973 (Grant Nos. 2011CB707903) from Ministry of Science and Technology, and National Science Foundation (Grant No. 81027006; 61020106008) China.

#### REFERENCES

- [1] J. Bercoff, "Supersonic shear imaging: a new technique for soft tissue elasticity mapping," IEEE Trans Ultrason Ferroelect Freq Control, 2004, vol. 51, pp. 396–409.
- [2] M. Tanter, "Quantitative assessment of breast lesion viscoelasticity: initial clinical results using supersonic shear imaging," Ultrasound Med Biol, 2008, vol. 34, pp. 1373–1386.
- [3] A. Athanasiou, "Breast lesions: quantitative elastography with supersonic shear imaging—preliminary results," Radiology, 2010, vol. 256, pp. 297–303.
- [4] W. A. Berg, "Shear-wave Elastography Improves the Specificity of Breast US: The BE1 Multinational Study of 939 Masses," Radiology, 2012, vol. 262, pp. 435–449.
- [5] A. Evans, "Quantitative shear wave ultrasound elastography: initial experience in solid breast masses," Breast Cancer Research, 2012, vol. 12:R104.
- [6] American College of Radiology. Breast Imaging Reporting and Data System (BI-RADS). Ultrasound. Reston, VA: American College of Radiology, 2003.
- [7] T. F. Chan, "Active contours without edges," IEEE Trans Image Processing, 2001, vol. 10, pp. 266–277.
- [8] W. K. Moon, "Analysis of elastographic and B-mode features at sonoelastography for breast tumor classification," Ultrasound Med Biol, 2009, vol. 35, pp. 1794–1802.
- [9] B. S. Garra, "Elastography of breast lesions: Initial clinical results," Radiology, 1997, vol. 202, pp. 79–86.